

Experimental exploration of novel semimetal state in strong anisotropic Pyrochlore iridate $\text{Nd}_2\text{Ir}_2\text{O}_7$ under high magnetic field

Z M Tian¹, Y Kohama¹, T Tomita¹, J Ishikawa¹, H Mairo¹, K Kindo¹, S Nakatsuji^{1,2}

¹ Institute for Solid State Physics, University of Tokyo, Kashiwa, Chiba 277-8581, Japan

² PRESTO, Japan Science and Technology Agency (JST), Kawaguchi, Saitama, 332-0012, Japan

E-mail: tianzhaoming@issp.u-tokyo.ac.jp

Abstract. We report the anisotropic magnetotransport of $\text{Nd}_2\text{Ir}_2\text{O}_7$ single crystal under high magnetic field (B) up to 50 T with B along various directions. Only for $B \parallel [001]$ direction, a novel semimetal state is realized under high magnetic field evidenced by a field-induced insulating-semimetallic phase transition with critical field $B_{\text{MI}} \sim 12$ T related to the destruction of all-in-all-out (AIAO) state. In contrast, abnormal magnetotransport hysteresis behavior is observed for $B \parallel [111]$ direction below the metal-insulator transition temperature (T_{MI}), and magnetotransport reveals the Ir spin structure keep in the AIAO state under high magnetic field with temperature just below T_{MI} , in prospect to realize Weyl semimetal state.

1. Introduction

Transition metal oxides (TMOs) of 5d elements have attracted a great deal of attention due to the interplay between a strong spin-orbit (SO) coupling and moderate electron correlation, providing a new platform for emergent electronic-or magnetic collective phenomena. Among these materials, pyrochlore iridates $R_2\text{Ir}_2\text{O}_7$ ($R = \text{Y}$, rare-earth element) are particular interest because various novel topological phases have been predicted to exist in certain correlation regimes, such as topological Mott insulator, Weyl semimetal (WSM) and axion insulator [1-4]. Experimental detection of this emergent topological phase should display anomalous Hall effect (AHE) and chiral magnetic effect [5,6], while these are still waiting for its experimental verification in spite of various theoretical proposals.

Most of $R_2\text{Ir}_2\text{O}_7$ compounds except for $R = \text{Pr}$ exhibit metal-insulator transition (MIT), as successive increasing ion radius of R ions causes the change from magnetic ordered insulators to a spin-disordered metal [7,8]. Near the transition from Mott insulating phase to the metallic ground state within the phase diagram, $\text{Nd}_2\text{Ir}_2\text{O}_7$ (Nd-227) shows significantly smaller MIT temperature with $T_{\text{MI}} \sim 32$ K, supporting a picture of Nd-227 residing at the boundary between correlated metal and insulator. Recent experiment on Nd-227 polycrystals suggests the nontrivial gapless metallic state localized at the AF domain wall [9]. Neutron diffraction experiments suggest the Ir^{4+} moments of Nd-227 consisting of an all-in-all-out (AIAO) magnetic structure as the ground state [10], where all the moments are pointing toward or outward from the center of each tetrahedron, leading to the coexistence of two kinds of antiferromagnetic (AF) domains namely all-in-all-out (A domain) and all-out-all-in (B domain) magnetic order [11]. These two configurations are not equivalent and are related by time-reversal symmetry, as the key ingredients to realize the predicted Weyl semimetal state [2]. Experimental investigation on single crystal would be highly desirable to unveil the emergent state due to the masked anisotropy effect of polycrystals, this will further lead us to realize the anisotropic control of spin texture and electronic structure by chemical (ionic radius of R) or physical pressure and



external magnetic field.

In this study, anisotropic magnetotransport on $\text{Nd}_2\text{Ir}_2\text{O}_7$ single crystals is reported with magnetic field along different directions including [111], [110] and [001] axis. Specially, a novel semimetal state under high magnetic field are suggested to be realized for $B // [001]$ direction by observation of MIT related to the destruction of AIAO state. For [111] direction, abnormal magnetoresistance hysteresis is observed for temperature below T_{MI} .

2. Experiment details

Single crystals of $\text{Nd}_2\text{Ir}_2\text{O}_7$ have been grown by a potassium fluoride-flux method. Powder and single crystal X-ray diffraction analyses show single phase and pyrochlore structure with lattice constant $a = 10.386(3)$ Å. Electron-probe microanalysis (EPMA) shows a slight deviation within 2% from stoichiometry in the Ir/Nd ratio for the single crystals.

The magnetotransport were measured by a standard four-probe method with current path along the [110] direction and magnetic field was always oriented perpendicular to the current direction with different typical magnetic field direction. DC resistivity measurement in a DC magnetic field were carried out using a commercial system (PPMS, Quantum Design) which has a base temperature of 2 K and highest magnetic field of 14 T. Electrical transport measurements up to 50 T in a pulsed high magnetic field were performed with frequency $f = 100$ kHz and electrical current $I = 280$ μA at the international megagauss laboratory at ISSP, the University of Tokyo. During the measurements, the electrical current was applied to [1-10] direction within the (100) plane. Field dependence of the magnetization in a field up to 14 T was measured using a commercial vibrating sample magnetometer system (PPMS, Quantum Design). Temperature dependence of magnetization was measured using a commercial SQUID (superconducting quantum interface device) magnetometer (MPMS, Quantum Design) in zero-field cooling and field cooling (FC) procedure from 2 to 300 K.

3. Results and discussion

Temperature dependence of resistivity for $\text{Nd}_2\text{Ir}_2\text{O}_7$ single crystal were measured under different magnetic field for B along [001] direction, as shown in Figure 1(a). The Metal-insulator (MI) transition temperature with $T_{\text{MI}} \sim 20$ K under zero field is lower than the value ~ 32 K observed in polycrystalline samples, most likely due to a carrier doping by slight off-stoichiometry around 2 %. The low resistivity of the zero-field cooling (ZFC) compared with the field cooling (FC) with 14T is attributed to the multi-domain wall state. Under magnetic field, the resistivity below T_{MI} was suppressed and become metallic state with $B = 14\text{T}$, this is consistent with field sweeping results at 2 K as shown in Figure 1(b), confirming the existence of field induced MIT behavior.

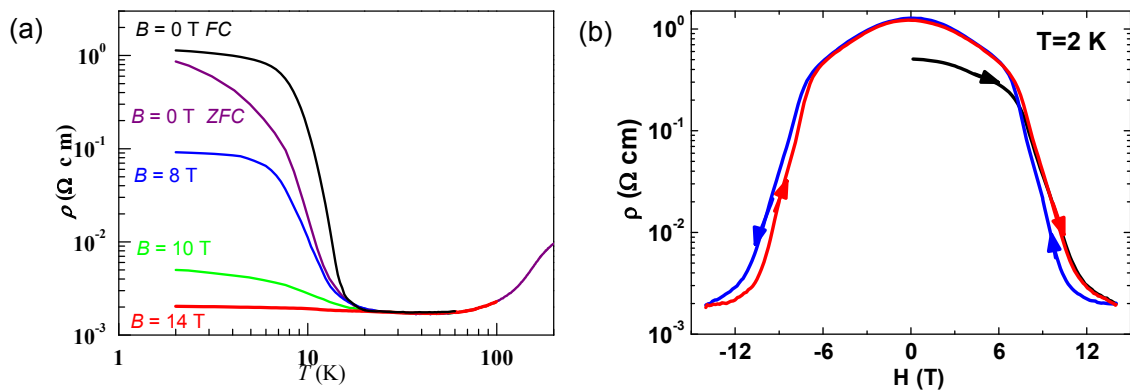


Figure 1 (a) Temperature dependence of resistivity measured under different magnetic field for $B // [001]$ direction, zero field cooling (ZFC) and field cooling under 14 T for $B = 0$ T; $B = 8$ T, 10 T and 14 T. (b) Field dependence of resistivity measured at 2 K for ZFC procedure.

To further clarify the field induced MI transition behavior, we measured the angle dependence of magnetoresistivity under pulsed magnetic field up to 50 T, presented in Figure 2(a). The field B was rotated within the (100) plane, perpendicularly to the current direction [1-10] with the angle (θ) between the field and the [001] direction as schematically shown in Figure 2(b) inset. In this definition, $\theta = 35^\circ$, $\theta = 55^\circ$ and $\theta = 90^\circ$ correspond to the field direction of [112], [111] and [110] axes, respectively. For field along these three axis directions, only a gradual decrease of the resistivity was found, revealing that the insulating state is stable up to 50 T. In sharp contrast, in the [001] direction, a rapid jump of the resistivity was observed at a critical field of $B_c = 12$ T above which, the resistivity becomes nearly constant. The magnetoresistance $[R(0)-R(B)]/R(B)$ amounts to 60,000 %. This sharp resistivity drop characterizes the field-induced phase transition to the high- B semimetal state. The narrow but clear hysteresis (~ 1 T) seen at the critical field indicates that the transition is first-order.

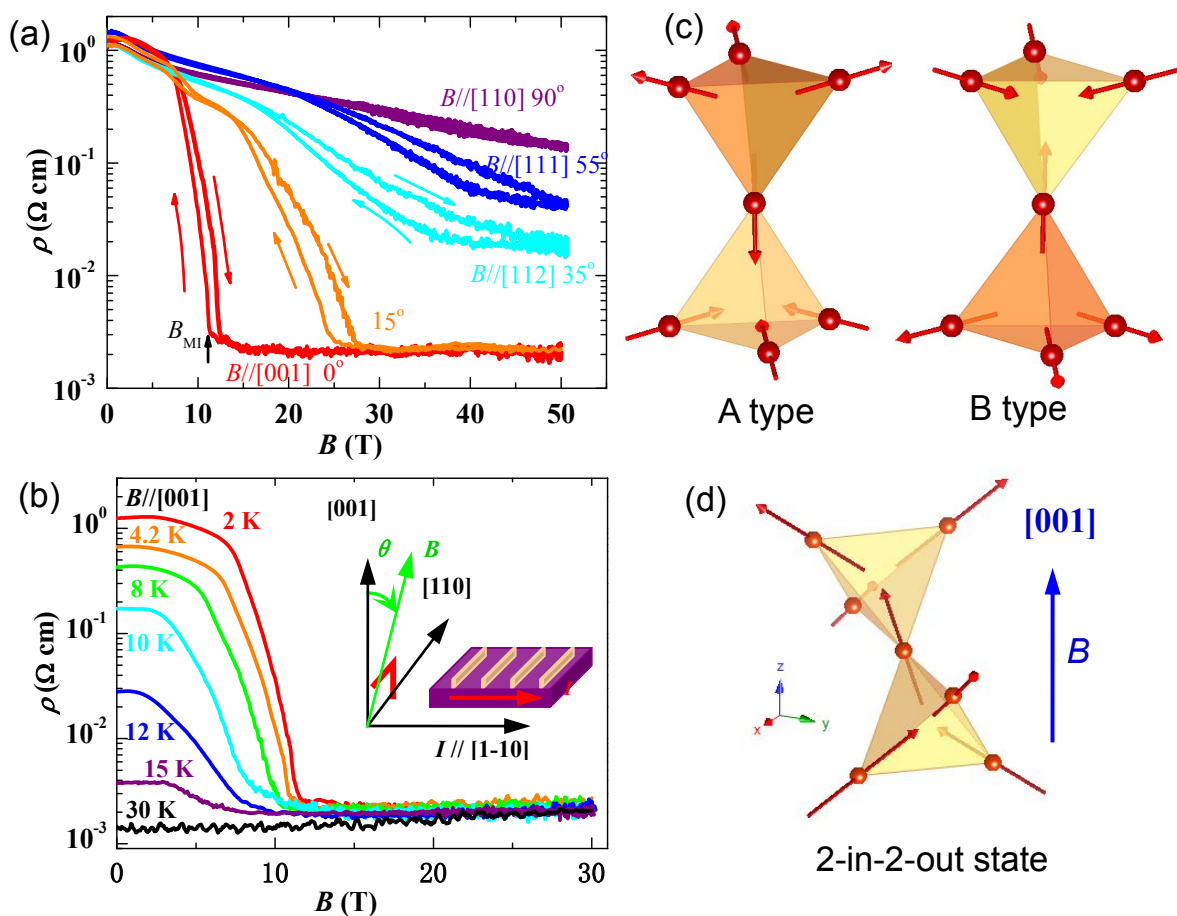


Figure 2 (a) Angle dependence of magnetoresistivity measured under pulsed magnetic field up to 50 T at 2 K with $I // [1-10]$ direction as shown in the inset of Figure 2 (b), (b) magnetoresistance measured at different temperatures from 2 K to 30 K; (c) All-in all-out domain state with A-type (AIAO) of domain(left) and B-type (AOAI) of domain (right); (d) 2-in-2-out domain with $B // [001]$ direction of Nd spin moments.

To map out the field-induced MIT, we show the resistivity versus field at various temperatures in Figure 2(b). The enhanced resistivity is confined to a region of small B and T , and outside this region, the resistivity is only weakly B and T dependent. Thus, there are simply two phases: an insulating antiferromagnetic state at small B and T , and a semimetallic state outside the ordered region. The

strong anisotropic magnetoresistance is also evident in the isothermal magnetization measured at 2 K shown in Figure 3(a). The magnetization for $B // [001]$ direction monotonically increases and then becomes saturated at 14 T, revealing the formation of 2-in-2-out state for Nd spin structure under high field as shown in Figure 2(d). Based on the neutron results [10,12], strong 4f-5d exchange interaction exists which set the Nd magnetic moment below 15 K to AIAO arrangement. Driven by the 4f-5d exchange interaction, the Nd spins polarization in the 2-in-2-out state will lead to the Ir magnetic moments to order in the same 2-in-2-out magnetic arrangement. In this case, the all-in-all-out (AIAO) AF order shown in Figure 2(c) becomes unstable, which lead to the field induced semi-metallic state at low field for the [001] orientation. This semimetal state corresponds to the destruction of AIAO spin configuration.

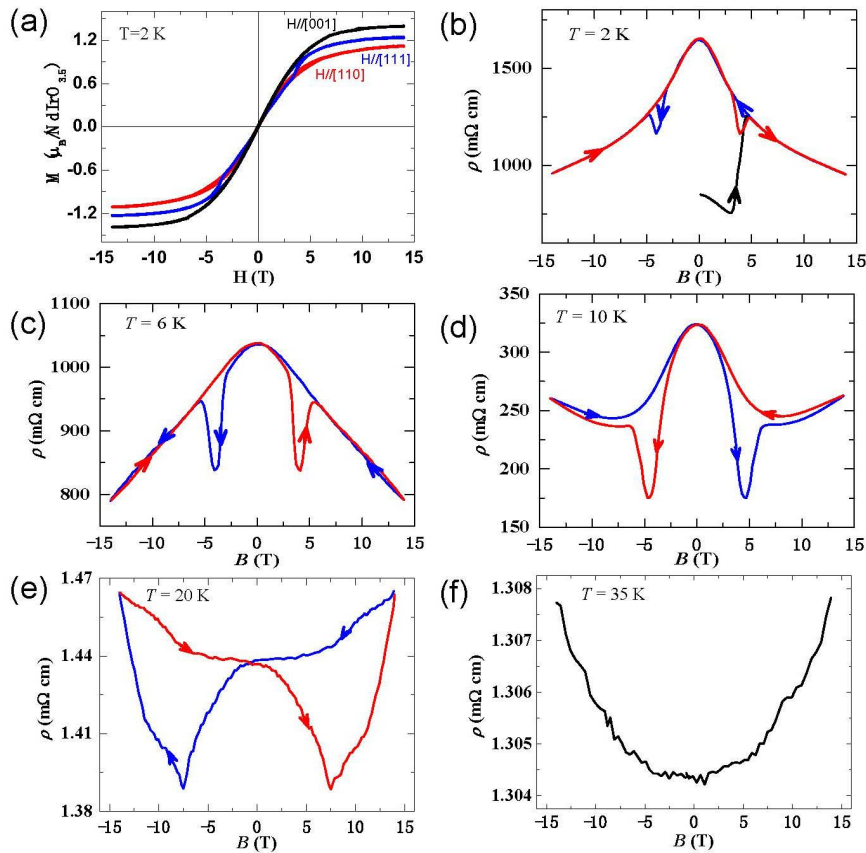


Figure 3 (a) Magnetization as a function of magnetic field at 2 K with magnetic field along the [111], [110] and [001] direction. (b-f) Field dependence of magnetoresistance for $B // [111]$ direction measured at different temperatures under ZFC cooling.

For $B // [111]$ seen from Figure 3(a), magnetic hysteresis is observed, while $M(B)$ is smooth for $B // [100]$ and [110]. In particular, the field derivative of the [111] magnetization curve reveals two distinct kinks around $B_{c1}=2.0$ T and $B_{c2}=3.9$ T (not shown here). Naively, these are suggestive of Nd^{3+} spin flops (the Ir moments are negligibly small on this scale [13]), which would arise in a classical “spin-ice” like Ising model [14]. Such a model (using the single-ion moment $2.4\mu_B/\text{Nd}$) predicts saturation at 1.4, 1.2, and $0.98\mu_B/\text{Nd}$ for B along [001], [111], and [110], consistent with 1.4, 1.2, and $1.1\mu_B/\text{Nd}$ in experiment. However, the smoothness of the sweeps for the [100] and [110] field orientations, as well as the fact that the down-sweep sequence shows no anomaly and reaches zero magnetization at zero field, are inconsistent with classical Ising spins.

Finally, we focus on magnetoresistance with $B // [111]$ direction at different temperatures in Figure 3(b-f). Compared to the [001] direction, no dramatic MIT is seen for $B // [111]$ at 2 K. Instead, the

[111] MR shows complex hysteresis corresponding to changes in the Nd spin structure [Figure 3(a)]. The results in the initial up-sweep process after ZFC shows a gradual decrease with field and spikes sharply, reaching a minimum value at 3.4 T. In the consecutive field cycles, the resistance exhibits dips at ± 3.9 T where the derivative of M peaks, revealing the close correlations between the MR and magnetization. Notably, the MR after the initial sweep forms a smooth curve interrupted only near the spin flop transition by a temporary dip. These observations can be understood in terms of two Ising domains of the AIAO order [Figure 2(c)] which can be aligned by a [111] field. Without such alignment, the initial zero-field state has multi-domains, and hence its lower resistivity can be attributed to more conductive domain walls [15]. This is also consistent with the dip in the spin flop region of the hysteresis loop, where again multi-domains are generated at this field.

For $B // [111]$ direction, we also note that positive magnetoresistance response is displayed under high magnetic field for $T > 10$ K compared with negative magnetoresistance at low temperatures ($T < 10$ K), Since the Nd moments freeze below 15 K [10], this difference can be attributed to the coupling energy difference between the 4f-5d magnetic moments. Below 10 K, the 3-in-1-out state of Nd spin structure is formed under high magnetic field, which will destruct the AIAO state of Ir spin structure leading to the negative magnetoresistance. As temperature increases up to 10 K, the 3-in-1-out state of Nd spin structure becomes unstable and 4f-5d exchange interaction become weak. Above 15 K, Nd spin moment keeps in the paramagnetic state, in this case, the AIAO spin structure of Ir moment only can switch between the all-in-all-out (A-type) domain and all-out-all-in (B-type) domain with the reversal of magnetic field as seen at 20 K, which preserve the all-in-all-out spin structure as a key ingredient to realize Weyl semimetal state. So, we argue that weyl semimetal state is expected to be existed only for $B // [111]$ direction.

4. Conclusion

The anisotropic magnetotransport of $\text{Nd}_2\text{Ir}_2\text{O}_7$ single crystal reveals that two ordered spin structures can be realized for B along [001] and [111] directions, suggesting the existence of two different semimetal state. Compared with [001] direction, weyl semimetal is suggested to be existed for $B // [111]$ direction just below MIT temperature due to the stability of AIAO state under high magnetic field.

Acknowledgement

We thank L. Balents, B. Kamran, Y Matsuo and T. Higo for useful discussions. This work was partially supported by a Grant-in-Aid for Scientific Research (No. 25707030) from the Japan Society for the promotion of Science (JSPS and by PRESTO, JST, Japan). Z.M. Tian acknowledges the financial support of the JSPS fellowship for foreign researchers (No. P14026).

References:

- [1] Pesin D and Balents L 2010 *Nat. Phys.* **6** 376
- [2] Wan X, Turner A M, Vishwanath A and Savrasov S Y 2011 *Phys. Rev B* **83** 205201
- [3] Burkov A A, Hook M D and Balents L 2011 *Phys. Rev B* **84** 235126
- [4] Witczak-Krempa W and Kim Y B 2012 *Phys. Rev B* **85** 045124
- [5] Machida Y, Nakatsuji S, Onoda S, Tayama T and Sakakibara T 2010 *Nature* **463** 210
- [6] Udagawa M and Moessner M 2013 *Phys. Rev. Lett* **111** 036602
- [7] Matsuhira K, Wakeshima M, Hinatsu Y and Takagi S 2011 *J. Phys. Soc. Jpn* **80** 094701
- [8] Nakatsuji S, Machida Y, Maeno Y, Tayama T, Sakakibara T, Van Duijin J, Balicas L, Millican J N, Macaluso R T, and Chan J Y 2006 *Phys. Rev. Lett* **96** 087204
- [9] Ueda, K, fujioka J, Takahashi Y, Suzuki T, Ishiwata S, Taguchi Y, Kawasaki M and Tokura Y 2014 *Phys. Rev B* **89** 075127
- [10] Tomiyasu, K, Matuhira K, Iwasa K, Watahiki M, Takagi S, Wakeshima M, Hinatsu Y, Yokoyama M, Ohoyama K and Yamada K 2012 *J. Phys. Soc. Jpn* **81** 034709
- [11] Arima, T 2013 *J. Phys. Soc. Jpn* **82** 013705

- [12] Ma E Y, Cui Y T, Ueda K, Tang S J, Chen K, Tamura N, Wu P M, Fujioka J, Tokura Y and Shen Z X 2015 *Science* **350** 538
- [13] Higashinaka R, Fukazawa H and Maeno Y 2003 *Phys. Rev B* **68** 014415
- [14] Shapiro M C, Riggs S C, Stone M B, De la Cruz C R, Chi S, Podlesnyak A A and Fisher I R 2012 *Phys. Rev B* **85** 214434
- [15] Yamaji Y and Imada M 2014 *Phys. Rev X* **4** 021035